

## Stat3 controls lysosomal-mediated cell death *in vivo*

Peter A. Kreuzaler<sup>1</sup>, Anna D. Staniszewska<sup>1</sup>, Wenjing Li<sup>1</sup>, Nader Omidvar<sup>2</sup>, Blandine Kedjouar<sup>1</sup>, James Turkson<sup>3</sup>, Valeria Poli<sup>4</sup>, Richard A. Flavell<sup>5</sup>, Richard W. E. Clarkson<sup>2</sup> and Christine J. Watson<sup>1,6</sup>

**It is well established that lysosomes play an active role during the execution of cell death<sup>1</sup>. A range of stimuli can lead to lysosomal membrane permeabilization (LMP), thus inducing programmed cell death without involvement of the classical apoptotic programme<sup>2,3</sup>. However, these lysosomal pathways of cell death have mostly been described *in vitro* or under pathological conditions<sup>4–7</sup>. Here we show that the physiological process of post-lactational regression of the mammary gland is accomplished through a non-classical, lysosomal-mediated pathway of cell death. We found that, during involution, lysosomes in the mammary epithelium undergo widespread LMP. Furthermore, although cell death through LMP is independent of executioner caspases 3, 6 and 7, it requires Stat3, which upregulates the expression of lysosomal proteases cathepsin B and L, while downregulating their endogenous inhibitor Spi2A (ref. 8). Our findings report a previously unknown, Stat3-regulated lysosomal-mediated pathway of cell death under physiological circumstances. We anticipate that these findings will be of major importance in the design of treatments for cancers such as breast, colon and liver, where cathepsins and Stat3 are commonly overexpressed and/or hyperactivated respectively<sup>1,9,10</sup>.**

Apoptosis is often used synonymously with the term programmed cell death, because many of the main cell death events have been identified as such. However, more recent work has shown that, particularly under circumstances in which cells have become refractory to apoptosis, other pathways leading to programmed cellular demise can be found<sup>4</sup>. In this context, the lysosomes play a crucial role and it is now well established that partial lysosomal membrane permeabilization (LMP) leads to relocalization of lysosomal components, such as cathepsins, to the cytosol, where they can act as executioner proteases<sup>11</sup>. Furthermore, an increasing number of stimuli including reactive oxygen species, calpains, sphingosine and the death receptor ligands tumour-necrosis factor (TNF) $\alpha$ , Fas and TNF-related weak inducer of apoptosis (TWEAK) have been identified as LMP-inducing agents<sup>11–15</sup>.

Nevertheless, the lysosomal-mediated pathway of cell death is still frequently believed to be just a backup mechanism when classical apoptotic stimuli fail to induce cell death.

Post-lactational regression (involution) of the mammary gland epithelium is one of the main cell death events in the adult mammalian organism. In rodents, the complete involution of the mammary gland to a near pre-pregnant state is accomplished within 10–15 days after weaning<sup>16</sup>. Studies over the past decade using genetically engineered mice have revealed critical upstream regulators of involution. These include soluble signalling molecules such as transforming growth factor- $\beta$  3 (TGF $\beta$ 3) and leukaemia inhibitory factor (LIF), transcription factors such as Stat3 and CCAAT/enhancer binding protein- $\delta$  (Cebp $\delta$ ) and remodelling enzymes such as matrix metalloproteases<sup>17–22</sup>. However, although presumed to be apoptosis, the modality of programmed cell death (PCD) during involution is not known. To investigate the mechanism of PCD *in vivo*, we carried out a morphological analysis of mammary gland involution in mice. This revealed several features that were atypical for classical apoptosis, such as two hypercondensed nuclei, swelling of the cells and a complete lack of membrane blebbing, while showing no features of a recently described form of PCD termed entosis, that has been discovered in mammary epithelial cells *in vitro*<sup>23</sup> (Fig. 1a). Furthermore, TdT-mediated dUTP nick end labelled (TUNEL) positive cells could not be detected in the first, reversible, phase of involution (0–2 days after weaning), whereas in the second, remodelling phase strong TUNEL staining was observed<sup>20</sup> (Fig. 1b and Supplementary Fig. S1). Despite traits of non-classical apoptotic PCD, executioner caspases are activated and cytochrome c is released from mitochondria during involution<sup>24</sup>. Closer inspection, however, revealed a temporal hierarchy of caspase activation in which caspases 3 and 6 are activated in both the first and second phases, whereas active caspase 7 was exclusively detected in the irreversible phase (Fig. 1c). Furthermore, in early involution, cleaved caspases 3 and 6 could be detected only in cells that had already been shed from the alveolar epithelium, whereas not a single cell positive for cleaved caspase 7 could be detected before day 3 of involution (Fig. 1d). To determine whether these caspases are required for PCD during this phase, we generated caspase 3 and 6 doubly

<sup>1</sup>Department of Pathology, University of Cambridge, Tennis Court Road, Cambridge CB2 1QP, UK. <sup>2</sup>School of Biosciences, University of Cardiff, Cardiff CF10 3US, UK. <sup>3</sup>University of Central Florida, 12722 Research Parkway, Orlando, Florida 32826, USA. <sup>4</sup>The Molecular Biotechnology Center (MBC), Department of Genetics, Biology and Biochemistry, University of Turin, 10126 Turin, Italy. <sup>5</sup>Section of Immunobiology, Yale University School of Medicine, New Haven, Connecticut 06520, USA. <sup>6</sup>Correspondence should be addressed to C.J.W. (e-mail: cjlw53@mole.bio.cam.ac.uk)

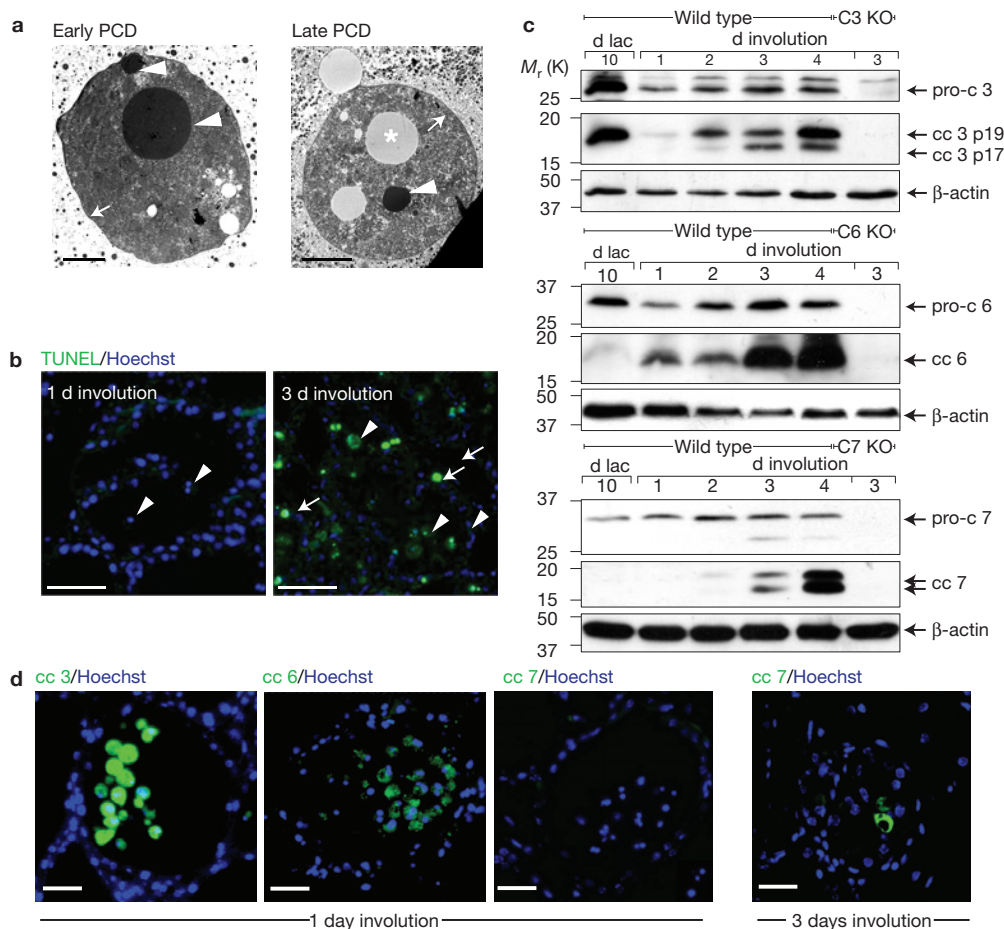


**Figure 1** Characteristics of physiological cell death in mammary gland involution. **(a)** Representative transmission electron micrographs of shed mammary epithelial cells in tissue from a 1 day involution time point at early and late stages of PCD, showing no blebbing (arrows) and hypercompacted nuclei (arrowheads; scale bars, 2  $\mu$ m; the asterisk marks a fat droplet). **(b)** TUNEL staining of mammary gland sections at 1 day and 3 days involution. At 1 day involution all cells including shed cells (arrowheads) are TUNEL negative. At 3 days involution many shed cells (arrowheads) and cells in the alveolar wall (arrows) are TUNEL positive (scale bars, 50  $\mu$ m). **(c)** Representative western blot analysis of at least three independent

biological samples showing pro- and cleaved caspases 3, 6 and 7 (pro-c and cc 3, 6 and 7, respectively) during lactation (lac) and involution with respective caspase-knockout (KO) tissue controls. Differential activation of the executioner caspases is apparent. **(d)** Immunohistochemical analysis of the occurrence of cleaved executioner caspases 3, 6 and 7 (cc 3, 6 and 7, respectively) during mammary gland involution. Cleaved caspases 3 and 6 can be detected in early involution, but are restricted to shed cells, whereas cleaved caspase 7 is detected only starting from 3 days of involution. Immunostaining of a single alveolus is shown for each image. Scale bars, 25  $\mu$ m. Uncropped images of blots are shown in Supplementary Fig. S9.

deficient mice (C3+6-knockout). Compensatory activation of caspase 7 did not occur in these mice, providing us with a system in which no executioner caspase was active (Fig. 2a–c). Surprisingly, involution progressed unabated, leading us to conclude that the cell death process in early involution is unlikely to rely on the activation of executioner caspases (Fig. 2d and Supplementary Fig. S2a). These findings were recapitulated in a doxycycline-inducible double-transgenic mouse strain overexpressing the viral caspase inhibitor p35 in the mammary gland under control of the mouse mammary tumour virus promoter<sup>25</sup> (Fig. 2e and Supplementary Fig. S2b).

Given the unusual morphology of PCD during involution as well as executioner caspase independence, we investigated alternative cell death mechanisms. We observed a striking downregulation of the structural lysosomal membrane protein LAMP2 in the mammary gland during lactation that persisted until the second day of involution (Fig. 3a). At a transcriptional level, both *Lamp2* and *Lamp1* messenger RNAs are downregulated during lactation (Supplementary Fig. S3).

Diminished LAMP expression has been suggested to sensitize cells to cell death by lysosomal leakage, which prompted us to investigate lysosomal-mediated PCD (LM-PCD; ref. 26). The cysteine cathepsins B and L were markedly upregulated with the onset of involution, which consequently translated into a striking increase in their activity (14-fold and 16-fold respectively; Fig. 3a,b and Supplementary Fig. S4a). This is in contrast to the aspartic cathepsin D, which has been shown to be only moderately active in the first phase of involution<sup>27</sup>. Immunohistochemical analysis revealed that, although cathepsin B mainly co-localized with LAMP2 during lactation, with the onset of involution this co-localization dropped sharply, which was reflected in a decreased Mander's coefficient (Fig. 3c,d).

To directly measure cathepsin activity in the cytoplasm of mammary epithelial cells during involution, we carried out subcellular fractionation of mammary tissue from lactation and involution time points. Strikingly, during lactation, over 95% of the total cathepsin B activity was found in the lysosomal fraction, but after

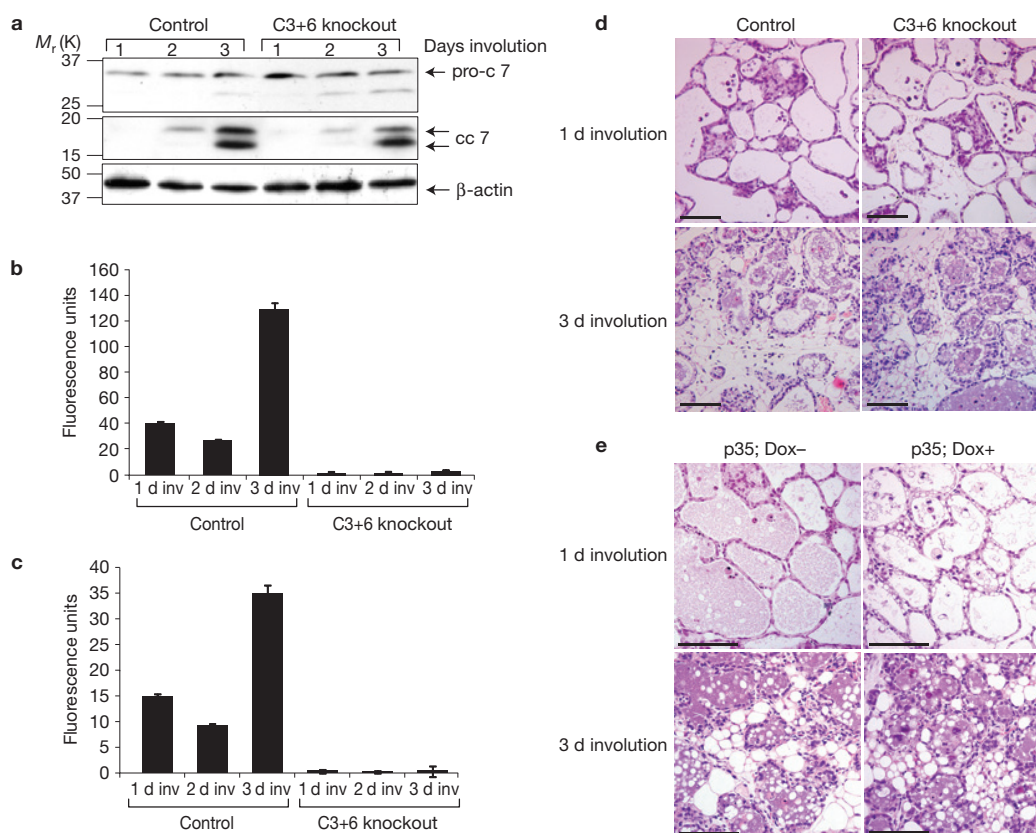


**Figure 2** Cell death in early involution is independent of executioner caspases. **(a)** Western blot analysis of caspase 7 in C3+6-knockout mice and wild-type controls during involution confirms lack of compensatory activation of caspase 7 in early involution. **(b,c)** Caspase activity was measured with the fluorescent substrates AC-DEVD-AMC for caspases 3 and 7 **(b)** and AC-VEID-AMC for caspase 6 **(c)**. In the caspase 3 and 6 double-knockout mice, no compensatory caspase 7 activation could be measured. The graphs show a representative time course; all values are means  $\pm$  s.d. of three independent

measurements. **(d)** Unabated progression of mammary gland involution in C3+6-knockout and wild-type control mice, shown on haematoxylin- and eosin-stained sections (scale bar, 100  $\mu$ m). **a–d** were carried out for five independent biological samples. **(e)** Unabated progression of mammary gland involution in p35-overexpressing mice after induction of the transgene by doxycycline, shown on haematoxylin- and eosin-stained sections representative of at least three independent biological repeats (scale bar, 100  $\mu$ m). Uncropped images of blots are shown in Supplementary Fig. S9.

only 24 h involution the activity was equally distributed between the cytoplasmic and lysosomal fractions. Cathepsin L activity was considerably increased, in addition to being redistributed to the cytoplasm during involution, with the lower cytosolic-to-lysosomal ratio, compared with cathepsin B, most probably being due to higher *de novo* synthesis of cathepsin L at this time point (Fig. 3e and Supplementary Fig. S4b,c). It is well established that cathepsins can not only leak into the cytosol, but also can be actively released into the intercellular space to degrade the extracellular matrix<sup>28</sup>. To ensure that the cathepsin activity in the cytosolic fraction did not merely originate from the extracellular space, we measured the leakiness of purified mammary lysosomes by incubation in a neutral buffer *in vitro*. During lactation, lysosomes lost very little cathepsin B and L, but with the onset of involution there was an almost complete loss of cathepsins from lysosomes within 90 min (Fig. 3f). This correlated with higher cathepsin B and L activity in the incubation buffer (Supplementary Fig. S5). Thus, during mammary gland involution, there is a marked increase in LMP, resulting in exodus of cathepsins B and L into the cytoplasm.

We have shown previously that Stat3 is essential for mammary epithelial cell PCD and subsequent involution<sup>19</sup> (Fig. 4a and Supplementary Fig. S6a,b). Using conditional Stat3<sup>fl/fl;BLG-Cre</sup> mice, in

which Stat3 is deleted exclusively from the mammary epithelium during lactation (hereafter called Stat3-knockout), we observed that during involution the protein and mRNA levels of both cathepsins B and L were considerably lower than time-matched Stat3<sup>fl/fl</sup> controls (hereafter called Stat3 controls; Fig. 4b,c). Moreover, subcellular fractionation revealed that the activity of cytosolic cathepsins B and L was 12 and seven times lower in the Stat3-knockout tissue respectively at 1 day involution and remained diminished throughout involution in both fractions (Fig. 4d,e). Conversely, stimulation of EPH4 mammary epithelial cells with oncostatin M (OSM), a cytokine that activates Stat3 during involution, led to a marked increase in cathepsin B and L protein levels and a more widespread cellular localization<sup>29</sup> (Fig. 4f,g). When co-incubating these cells with cycloheximide, an accumulation of *cathepsin b* mRNA could be detected, arguing for transcriptional control downstream of OSM without the need for protein synthesis (Fig. 4h). Furthermore, staining these cells with the lysosomotropic dye LysoTracker Red showed that after treatment with OSM, EPH4 cells undergo LMP, as can be seen by the appearance of a population of cells with low LysoTracker intensities (Fig. 4i,j). Taken together, this shows the direct involvement of Stat3 in the regulation of the expression of cysteine cathepsins and their localization.

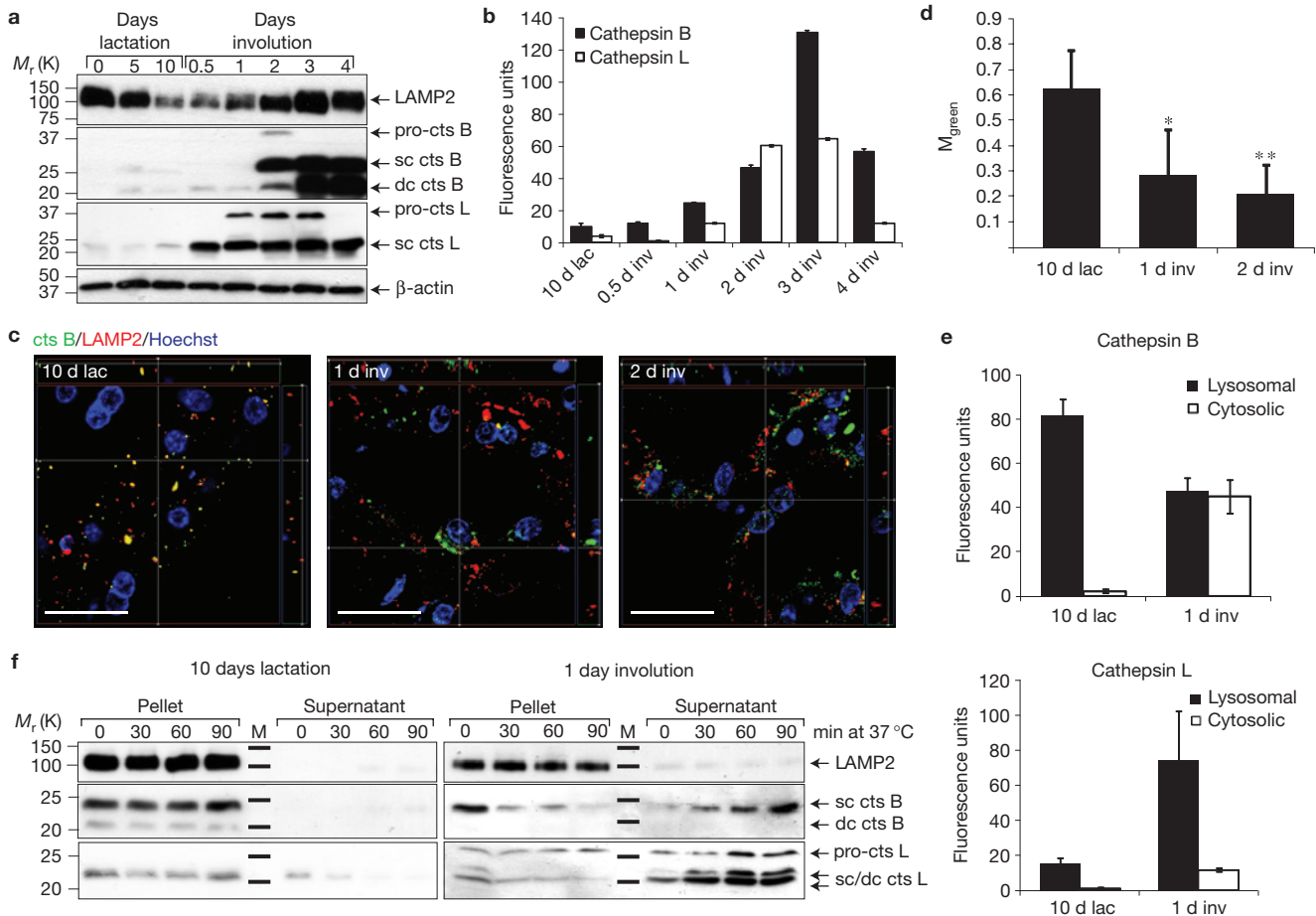


**Figure 3** Mammary lysosomes become leaky during involution. **(a)** Western blot showing decrease of LAMP2 during lactation and early involution and increase of cathepsin B and L (cts B and L; sc, single chain, dc, heavy chain of the double-chain form; both the single-chain and the double-chain form are active) in involution. **(b)** Increasing cathepsin B and L activity in whole gland lysates during lactation and involution was measured by cleavage of the fluorescent substrate Z-Phe-Arg-AMC. Error bars represent the standard deviation of measurements from three independent biological samples. **(c)** Immunohistochemical analysis of the subcellular localization of cathepsin B (green) with respect to the lysosomal marker LAMP2 (red) in lactation and involution time points. A decreased co-localization during involution is apparent. Nuclei stained with Hoechst (scale bars, 20  $\mu$ m). **(d)** Mander's coefficient of co-localization for cathepsin B (green) with respect to LAMP2 (red) was determined for three biological repeats in

at least 15 focal planes per section. A sharp decrease is apparent in involution time points ( $*P < 0.05$ ,  $**P < 0.01$  as determined by Student's *t*-test,  $n = 3$ ). **(e)** Increase in cytosolic cathepsin B and L activity was measured after subcellular fractionation of mammary gland samples from lactation and involution time points. The data are the average of three biological repeats. All values are means  $\pm$  s.d. **(f)** Increased leakiness of purified mammary lysosomes from a 1 day involution time point, compared with a 10 day lactation time point, shown by incubation of the lysosomes in a neutral buffer at 37  $^{\circ}$ C for the indicated time. After re-pelleting, the amounts of cathepsins B and L retained in the lysosomes as well as the amounts leaked into the supernatant, were assessed by immunoblotting, with LAMP2 as a lysosomal marker. All of the above were carried out with at least three independent biological samples. All values are means  $\pm$  s.d. Uncropped images of blots are shown in Supplementary Fig. S9.

With the onset of involution, we observed a sharp, LMP-mediated decline in lysosomal cathepsin B activity in all mice studied (Figs 3e and 4d). Although lysosomal leakiness and concomitant loss of lysosomal cathepsin B activity is unchanged in the Stat3-knockout glands, a corresponding increase in cytosolic cathepsin activity was not apparent (Fig. 4d, compare lanes 0.5 and 1 day inv in left and right panels). This implies that Stat3 does not affect the leakiness of the lysosomes *per se*, but rather diminishes cytosolic cathepsin activity by some mechanism in addition to transcriptional regulation of cathepsin gene expression.

Serpins are a large class of suicide protease inhibitors. Members of this family that are specific for cysteine cathepsins, such as Spi2A in mice and SRP-6 in *Caenorhabditis elegans*, have been shown to protect against cathepsin-mediated cell death in memory T cells and after toxic insults respectively<sup>6,30</sup>. Analysis of microarray data from a mammary

developmental time course revealed that mRNA for Spi2A (encoded by *Serpina3g*; ref. 31) was highly induced during lactation<sup>32</sup>. Spi2A mRNA expression was maximal at day 10 lactation, at the time when LAMP2 was downregulated, and dropped precipitously with the onset of involution, whereas clade B serpins had inverse expression profiles (Figs 3a and 5a and Supplementary Fig. S7a). This is congruent with its function as a cathepsin inhibitor and safeguard mechanism against LM-PCD. Strikingly, the Stat3-knockout mice show strong transcriptional upregulation of Spi2A (up to 200-fold) throughout involution, thus explaining the lack of cytosolic cathepsin activity measured in Stat3-deficient mammary tissue (Figs 5b and 4d,e). Interestingly, although the upstream flanking *Serpina3f* is regulated in a similar manner, this is not the case for the downstream flanking *Serpina3h*, arguing against a generalized activation of the serpin locus (Supplementary Fig. S7b,c).

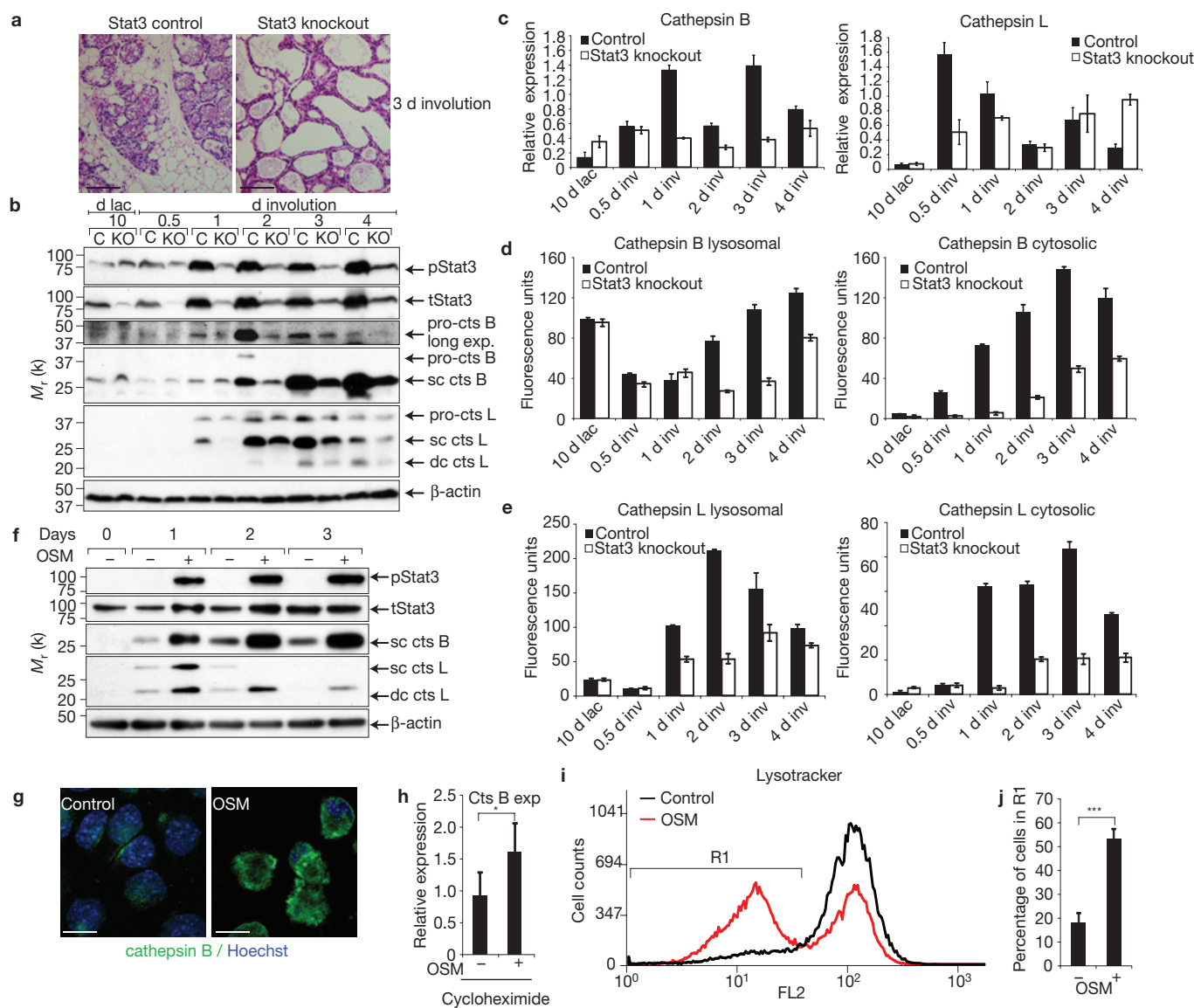


**Figure 4** Stat3 regulates cathepsin B and L expression. **(a)** Delay of mammary gland involution in Stat3-knockout mice, compared with Stat3 control mice, shown by haematoxylin- and eosin-stained sections (scale bar, 100  $\mu$ m). **(b)** Reduced amounts of total and tyrosine-phosphorylated Stat3 (tStat3; pStat3) and cathepsins B and L (cts B, L; sc, single chain, dc, heavy chain of the double-chain form) in Stat3-knockout (KO), when compared with control (C), mice shown by western blotting. **(c)** Reduced expression of *cathepsin b* and *cathepsin l* in Stat3-knockout mice measured by quantitative real-time PCR relative to *cyclophilin a*. **(d,e)** Reduced lysosomal (after 2 days involution) and cytosolic (throughout involution) activity of cathepsins B and L in Stat3-knockout mice when compared with Stat3 controls, shown by subcellular fractionation and subsequent cathepsin activity measurement. All values above are means  $\pm$  s.d. for three independent measurements and are representative of three independent biological repeats. **(f)** The mammary epithelial cell line EPH4 was stimulated with OSM (25 ng ml<sup>-1</sup>) or carrier (0.0001% BSA in PBS) for the indicated time. Increased tyrosine-phosphorylation of Stat3

and concomitant increase of cathepsins B and L are shown by western blot. **(g)** EPH4 cells were stimulated as in **f** for 3 days. Cells were subsequently fixed and stained for cathepsin B (green). The cells were analysed by deconvolution microscopy and show a redistribution of cathepsin B from a perinuclear localization to a diffused pattern throughout the cytosol (scale bar, 25  $\mu$ m). **(h)** EPH4 cells were co-stimulated with OSM (25 ng ml<sup>-1</sup>) and cycloheximide (10  $\mu$ g ml<sup>-1</sup>) for 6 h and the mRNA levels for *cathepsin b* were analysed by quantitative real-time PCR. An increase in *cathepsin b* mRNA is apparent after OSM stimulation. Values are means  $\pm$  s.d. from three independent biological repeats (\**P* < 0.05, as determined by Student's *t*-test). **(i)** Representative plot of EPH4 cells treated as in **f** for 3 days and subsequently stained with the lysosomotropic dye LysoTracker Red (Invitrogen, 100 nM). OSM-treated cells showed a population of reduced staining, resulting from LMP. **(j)** Quantification of three independent experiments as described in **i** (\*\*\*) *P* < 0.001, as determined by Student's *t*-test; values are means  $\pm$  s.d.). Uncropped images of blots are shown in Supplementary Fig. S9.

To mimic the inhibition of cathepsin activity by high Spi2A levels in the Stat3-knockout mice, we injected Stat3 control mice with the cell permeable cathepsin B inhibitor CA-074Me. After three days of treatment, we observed a substantial delay in the regression of the mammary gland, compared with vehicle-injected controls. Notably,

the extent of cathepsin B inhibition correlated strongly with the delay in regression, demonstrating a crucial role for cathepsin B in involution. (*r* = 0.97, Fig. 5c,d.)

Finally, using EPH4 mammary epithelial cells, we could effectively induce cell death by stimulation with OSM to activate Stat3, as occurs in

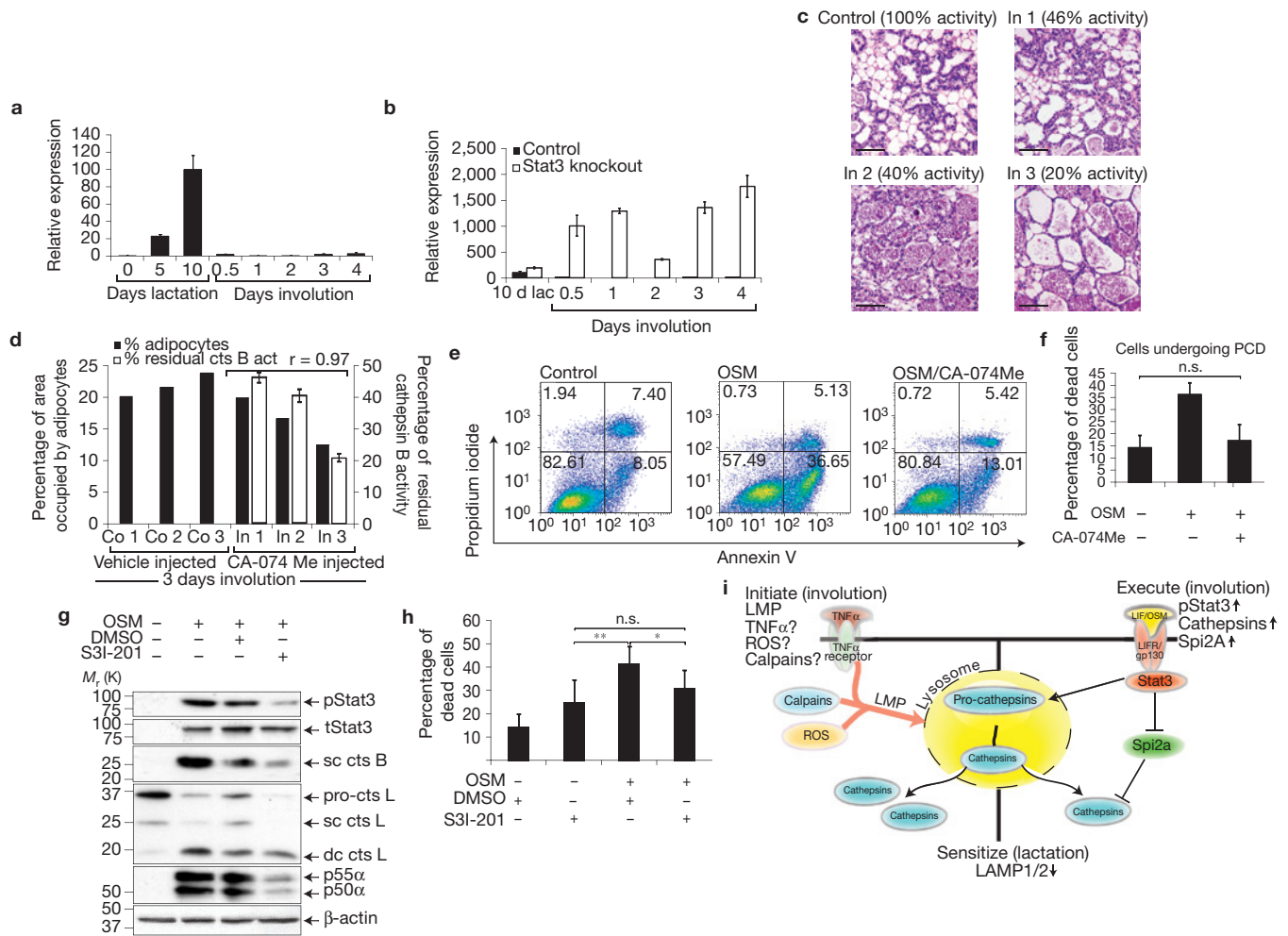


**Figure 5** Inhibition of cytosolic cathepsin activity prevents Stat3-mediated cell death. **(a)** Expression of *spi2a* is high in lactation and drops in involution, as shown by quantitative real-time PCR relative to *cyclophilin a* expression in wild-type mice. **(b)** Expression of *spi2a* further increases during involution in Stat3-knockout mice (graphs normalized to respective samples at 10 days lactation; values in **a** and **b** represent means  $\pm$  s.d. for three independent measurements and are representative of three independent biological samples). **(c,d)** Mice were administered 40 mg kg<sup>-1</sup> of the cathepsin B inhibitor CA-074Me (In, inhibitor-injected mice). **(c)** Representative micrographs showing the delay in involution (scale bar, 100  $\mu$ m). **(d)** Delayed involution on cathepsin B inhibition is apparent when quantifying the area occupied by adipocytes. The delay correlates with the extent of inhibition as expressed by the Pearson coefficient ( $r = 0.97$ ). The values represent individual mice. Values of white bars represent means  $\pm$  s.d. **(e,f)** Treatment of EPH4 cells with OSM (25 ng ml<sup>-1</sup>) for 72 h efficiently induces cell death, which can be abrogated by the cathepsin B inhibitor CA-074Me (10  $\mu$ M).

Cell death was assessed with Annexin V/propidium iodide co-staining and flow cytometry. **(e)** Representative dot plots for each treatment; **(f)** quantification of total cell death in three independent experiments. Values represent means  $\pm$  s.d. of three independent biological repeats. There was no significant (n.s.) difference between control samples and samples treated with OSM and CA-074Me as determined by Student's *t*-test. **(g)** EPH4 cells were stimulated with OSM (25 ng ml<sup>-1</sup>), whereas Stat3 was inhibited with the small-molecule inhibitor S3I-201 (50  $\mu$ M). Immunoblotting confirmed reduced phosphorylated Stat3 on inhibitor treatment, as well as reduction of cathepsins B and L and the established Stat3 target p50 $\alpha$ /p55 $\alpha$ . **(h)** Cell death was measured as in **e** with inhibition of Stat3 with S3I-201 (50  $\mu$ M). Cell death was reduced to levels similar to those seen with the inhibitor alone, showing a protective effect of Stat3 inhibition. All values represent means  $\pm$  s.d. for a minimum of three independent experiments. Uncropped images of blots are shown in Supplementary Fig. S9. **(i)** Proposed model of the findings, in which Stat3 is needed for the execution of LM-PCD. Further details in the text.

involution. Abrogation of cathepsin B activity with CA-074Me reduced cell death to background levels, whereas the pan-caspase inhibitor z-VAD-FMK showed almost no effect (Fig. 5e,f and Supplementary Fig. S8). Moreover treatment of OSM-stimulated EPH4 cells with a small-molecule Stat3 inhibitor (S3I-201) decreased protein levels of cathepsins B and L and reduced cell death significantly (Fig. 5g,h). Thus, we could recapitulate our *in vivo* findings in mammary epithelial cells in culture.

We have previously shown that the NF- $\kappa$ B pathway is activated during mammary gland involution, and Spi2A is a

known target of NF- $\kappa$ B in memory T cells<sup>8,33</sup>. As Stat3 can block the transcription of NF- $\kappa$ B targets by binding to, and inhibiting, p65/p50 subunits<sup>34</sup>, we propose that abrogating Stat3 signalling in Stat3-knockout mice will abolish the inhibitory effect of Stat3 on the NF- $\kappa$ B pathway, promoting strong overexpression of Spi2A. This would give Stat3 an important role in modulating NF- $\kappa$ B signalling, favouring a cell death rather than a survival signature.

Taken together, we have shown that during involution of the mammary gland, epithelial cells undergo a lysosomal-dependent PCD,

which is independent of executioner caspases. To our knowledge this is the first time that this cell death mechanism has been described under physiological conditions, which calls for reassessment of other cell death events in which caspases might be activated not as a cause, but as a consequence, of PCD. Our data indicate a multistep process leading to LM-PCD (Fig. 5i). In the first stage, during lactation, the cells may become sensitized to LMP by the downregulation of the lysosomal membrane proteins LAMP1 and 2. This is followed by the initiation of LMP, by signals that have yet to be defined. However, TNF $\alpha$  signalling and elevated Ca<sup>2+</sup> levels, both occurring during early involution, have been shown to induce LMP (refs 2,35,36). The third step in LM-PCD can be termed the execution of LMP, because LMP alone does not seem to kill cells efficiently. This is accomplished by Stat3 in at least two ways: (1) by upregulating levels of cathepsins B and L, which are known to act as executioner proteases when in the cytosol, and (2) by downregulating transcription of the endogenous cysteine cathepsin inhibitor Spi2A.

Our findings show a mechanism for Stat3-mediated cell death and reveal a direct connection between Stat3, cysteine cathepsins and LM-PCD. Paradoxically, Stat3 is constitutively activated in a number of different cancers and elevated levels of cathepsin B have been shown to promote metastasis<sup>10,37</sup>. Elucidation of how tumour cells with chronic activation of Stat3 evade this type of cell death is likely to reveal new, more directed, targets for therapeutic purposes. □

## METHODS

Methods and any associated references are available in the online version of the paper at <http://www.nature.com/naturecellbiology/>

Note: Supplementary Information is available on the Nature Cell Biology website

## ACKNOWLEDGEMENTS

We thank J. Skepper for help with the electron microscopy and B. Potter for histological preparations. We thank also P. Came for the TUNEL data and W. Khaled for discussions. This work has been supported by a PhD studentship from the Pathology Department, University of Cambridge (P.A.K.), Breast Cancer Campaign PhD studentship (A.D.S. and W.L.), Italian Cancer Research Association (V.P.) and Biotechnology and Biological Sciences Research Council grant no. BB/C006836/1 (R.W.E.C. and N.O.).

## AUTHOR CONTRIBUTIONS

P.A.K. carried out project design and all experiments, except those stated separately and wrote the manuscript; A.D.S. designed and carried out the *in vitro* studies; W.L. carried out studies on caspase-knockout mice; N.O. and R.W.E.C. generated the p35 transgenic mouse and provided data; B.K. carried out caspase studies; J.T. provided Stat3 inhibitor; V.P. provided Stat3<sup>fl/fl</sup> mice; R.A.F. provided all caspase-knockout mice; C.J.W. carried out project design and wrote the manuscript.

## COMPETING FINANCIAL INTERESTS

The authors declare no competing financial interests.

Published online at <http://www.nature.com/naturecellbiology>

Reprints and permissions information is available online at <http://npg.nature.com/reprintsandpermissions/>

- Kroemer, G. & Jaattela, M. Lysosomes and autophagy in cell death control. *Nat. Rev. Cancer* **5**, 886–897 (2005).
- Guicciardi, M. E., Leist, M. & Gores, G. J. Lysosomes in cell death. *Oncogene* **23**, 2881–2890 (2004).
- Hitomi, J. *et al.* Identification of a molecular signaling network that regulates a cellular necrotic cell death pathway. *Cell* **135**, 1311–1323 (2008).
- Lockshin, R. A. & Zakeri, Z. Caspase-independent cell death? *Oncogene* **23**, 2766–2773 (2004).
- Nylandsted, J. *et al.* Eradication of glioblastoma, and breast and colon carcinoma xenografts by Hsp70 depletion. *Cancer Res.* **62**, 7139–7142 (2002).

- Luke, C. J. *et al.* An intracellular serpin regulates necrosis by inhibiting the induction and sequelae of lysosomal injury. *Cell* **130**, 1108–1119 (2007).
- Guicciardi, M. E., Miyoshi, H., Bronk, S. F. & Gores, G. J. Cathepsin B knockout mice are resistant to tumor necrosis factor- $\alpha$ -mediated hepatocyte apoptosis and liver injury: implications for therapeutic applications. *Am. J. Pathol.* **159**, 2045–2054 (2001).
- Liu, N. *et al.* NF- $\kappa$ B protects from the lysosomal pathway of cell death. *EMBO J.* **22**, 5313–5322 (2003).
- Grivnenikov, S. *et al.* IL-6 and Stat3 are required for survival of intestinal epithelial cells and development of colitis-associated cancer. *Cancer Cell* **15**, 103–113 (2009).
- Vasiljeva, O. *et al.* Reduced tumour cell proliferation and delayed development of high-grade mammary carcinomas in cathepsin B-deficient mice. *Oncogene* **27**, 4191–4199 (2008).
- Foghsgaard, L. *et al.* Cathepsin B acts as a dominant execution protease in tumor cell apoptosis induced by tumor necrosis factor. *J. Cell Biol.* **153**, 999–1010 (2001).
- Holler, N. *et al.* Fas triggers an alternative, caspase-8-independent cell death pathway using the kinase RIP as effector molecule. *Nat. Immunol.* **1**, 489–495 (2000).
- Kagedal, K., Zhao, M., Svensson, I. & Brunk, U. T. Sphingosine-induced apoptosis is dependent on lysosomal proteases. *Biochem. J.* **359**, 335–343 (2001).
- Nakayama, M. *et al.* Multiple pathways of TWEAK-induced cell death. *J. Immunol.* **168**, 734–743 (2002).
- Yamashima, T. Implication of cysteine proteases calpain, cathepsin and caspase in ischemic neuronal death of primates. *Prog. Neurobiol.* **62**, 273–295 (2000).
- Lascelles, A. K. & Lee, C. S. *Lactation: A Comprehensive Treatise* Vol. 4. (Academic, 1978).
- Nguyen, A. V. & Pollard, J. W. Transforming growth factor  $\beta$ 3 induces cell death during the first stage of mammary gland involution. *Development* **127**, 3107–3118 (2000).
- Kritikou, E. A. *et al.* A dual, non-redundant, role for LIF as a regulator of development and STAT3-mediated cell death in mammary gland. *Development* **130**, 3459–3468 (2003).
- Chapman, R. S. *et al.* Suppression of epithelial apoptosis and delayed mammary gland involution in mice with a conditional knockout of Stat3. *Genes Dev.* **13**, 2604–2616 (1999).
- Lund, L. R. *et al.* Two distinct phases of apoptosis in mammary gland involution: proteinase-independent and -dependent pathways. *Development* **122**, 181–193 (1996).
- Thangaraju, M. *et al.* C/EBP  $\delta$  is a crucial regulator of pro-apoptotic gene expression during mammary gland involution. *Development* **132**, 4675–4685 (2005).
- Baxter, F. O., Neoh, K. & Tevendale, M. C. The beginning of the end: death signaling in early involution. *J. Mamm. Gland Biol. Neoplasia* **12**, 3–13 (2007).
- Overholtzer, M. *et al.* A nonapoptotic cell death process, entosis, that occurs by cell-in-cell invasion. *Cell* **131**, 966–979 (2007).
- Marti, A. *et al.* Mouse mammary gland involution is associated with cytochrome c release and caspase activation. *Mech. Dev.* **104**, 89–98 (2001).
- Zhou, Q. *et al.* Interaction of the baculovirus anti-apoptotic protein p35 with caspases. Specificity, kinetics, and characterization of the caspase/p35 complex. *Biochemistry* **37**, 10757–10765 (1998).
- Fehrenbacher, N. *et al.* Sensitization to the lysosomal cell death pathway by oncogene-induced down-regulation of lysosome-associated membrane proteins 1 and 2. *Cancer Res.* **68**, 6623–6633 (2008).
- Zaragoza, R. *et al.* Nitration of cathepsin D enhances its proteolytic activity during mammary gland remodelling after lactation. *Biochem. J.* **419**, 279–288 (2009).
- Mohamed, M. M. & Sloane, B. F. Cysteine cathepsins: multifunctional enzymes in cancer. *Nat. Rev. Cancer* **6**, 764–775 (2006).
- Tiffen, P. G. *et al.* A dual role for oncostatin M signaling in the differentiation and death of mammary epithelial cells *in vivo*. *Mol. Endocrinol.* **22**, 2677–2688 (2008).
- Liu, N. *et al.* Serine protease inhibitor 2A is a protective factor for memory T cell development. *Nat. Immunol.* **5**, 919–926 (2004).
- Inglis, J. D. & Hill, R. E. The murine Spi-2 proteinase inhibitor locus: a multigene family with a hypervariable reactive site domain. *EMBO J.* **10**, 255–261 (1991).
- Clarkson, R. W., Wayland, M. T., Lee, J., Freeman, T. & Watson, C. J. Gene expression profiling of mammary gland development reveals putative roles for death receptors and immune mediators in post-lactational regression. *Breast Cancer Res.* **6**, R92–R109 (2004).
- Clarkson, R. W. *et al.* NF- $\kappa$ B inhibits apoptosis in murine mammary epithelia. *J. Biol. Chem.* **275**, 12737–12742 (2000).
- Yu, Z., Zhang, W. & Kone, B. C. Signal transducers and activators of transcription 3 (STAT3) inhibits transcription of the inducible nitric oxide synthase gene by interacting with nuclear factor  $\kappa$ B. *Biochem. J.* **367**, 97–105 (2002).
- Baxter, F. O. *et al.* IKK $\beta$ /2 induces TWEAK and apoptosis in mammary epithelial cells. *Development* **133**, 3485–3494 (2006).
- Reinhardt, T. A. & Lippolis, J. D. Mammary gland involution is associated with rapid down regulation of major mammary Ca<sup>2+</sup>-ATPases. *Biochem. Biophys. Res. Commun.* **378**, 99–102 (2009).
- Yu, H., Pardoll, D. & Jove, R. STATs in cancer inflammation and immunity: a leading role for STAT3. *Nat. Rev. Cancer* **9**, 798–809 (2009).

## METHODS

**Animal husbandry.** Mice carrying the *stat3* gene flanked by *loxP* sites<sup>38</sup> were crossed with a strain containing a  $\beta$ -lactoglobulin-promoter-driven Cre gene<sup>39</sup> (both on a mixed background). Caspase 3, 6 and 7 mice<sup>40–42</sup> are on a C57BL/6 background. Mice with a doxycycline-inducible p35 transgene are on the FVB background. Transgenic induction was achieved with the administration of 2 mg ml<sup>-1</sup> doxycycline (Sigma) in the drinking water for 7 days accompanied by intraperitoneal injection (5 mg kg<sup>-1</sup>) for 5 days before collection. C57BL/6 mice were purchased from Harlan labs. The mice were bred in regular cages with food and water *ad libitum*. Virgin female mice, 8–14 weeks old, were mated and males were subsequently removed before birth to avoid second pregnancies. Dams were killed at indicated time points. For involution studies, pups were removed at 10 days of lactation. At least three mice were used for each time point in every experiment. All animals were treated according to local ethical committee and the UK Home Office guidelines and killed through CO<sub>2</sub> or dislocation of the neck.

**Cathepsin B inhibition *in vivo*.** Stat3 control mice were mated as described above and pup numbers were normalized to eight. At day 10 of lactation, the pups were removed and the mice were administered 40 mg kg<sup>-1</sup> CA-074Me (Peptanova, 5 mg dissolved in 80  $\mu$ l dimethylsulphoxide and 1,520  $\mu$ l PBS) by intraperitoneal injection every 12 h. Control mice received vehicle alone. After 3 days the mice were euthanized and the glands were fixed and analysed.

**Assessment of delayed involution *in vivo*.** To quantify the delay of mammary gland involution following cathepsin B inhibition, the area occupied by adipocytes was assessed on haematoxylin- and eosin-stained mammary gland sections using ImageJ software. The mean activity of the control mice was set as 100% and the amounts of residual cathepsin B activity were related to this value. The correlation was tested with the Pearson coefficient.

**Transmission electron microscopy.** Transmission electron microscopy was carried out as previously described<sup>43</sup>.

**Haematoxylin and eosin staining.** Haematoxylin and eosin staining was carried out as previously described<sup>44</sup>.

**TUNEL staining of mammary gland sections.** The reaction was carried out on fixed tissues using the ApoTag indirect fluorescence staining kit (S7110, Chemicon) following the manufacturer's instructions.

**Subcellular fractionation.** Lymph node divested number four glands were homogenized (approximately 15 strokes) in a tight-fitting handheld homogenizer in 1 ml of subcellular fractionation buffer (HEPES-KOH 20 mM, sucrose 250 mM, KCl 10 mM, MgCl<sub>2</sub> 1.5 mM, EDTA 1 mM, EGTA 1 mM, dithiothreitol 8 mM, Pefabloc 1 mM (Fluka), at pH 7.5). Debris and nuclei were pelleted at 750g (3,500 r.p.m., BeckmanCoulter Optima L-100 XP Ultracentrifuge, 4°C) for 12 min. The supernatant was spun at 10,000g (12,900 r.p.m.) for 35 min to pellet lysosomes and other organelles. The pellet was rinsed and collected in 300 ml subcellular fractionation buffer as lysosomal fraction. The supernatant, containing cytosolic and extracellular components, was cleared of microsomes by an extra spin at 100,000g (40,000 r.p.m.) for 1 h and collected as cytosolic fraction. Organelles were disrupted by three cycles of freezing and thawing.

**Lysosomal-leakiness assay.** Lysosomes from two whole mammary glands excluding lymph nodes were prepared as described, with the exception that the subcellular fractionation buffer was made up with Complete protease inhibitor (Roche) instead of Pefabloc (subcellular fractionation protease inhibitor). They were washed once in subcellular fractionation buffer and re-pelleted in a table-top centrifuge (Heraeus Fresco-17 centrifuge, 4°C, 15 min, 12,000 r.p.m., 13, 800g). After resuspending in 400  $\mu$ l subcellular fractionation protease inhibitor buffer, equal volumes (50  $\mu$ l) were either pelleted immediately or incubated for the indicated time at 37°C under gentle agitation. Subsequently, the lysosomes were re-pelleted as above. The supernatant was removed and snap frozen. The pellet was resuspended in 150  $\mu$ l RIPA buffer (50 mM Tris, 1% NP40, 0.25% sodium deoxycholate, 150 mM NaCl, 1 mM EGTA and Complete protease inhibitor), and organelles were lysed on ice for 30 min with intermittent vortexing. Membranes were pelleted in a table-top centrifuge (Heraeus Fresco-17 centrifuge, 4°C, 15 min, 12,000 r.p.m., 13, 800g), the supernatant was removed and equal amounts of the resuspended pellet and the supernatant were analysed by western blot.

**Cathepsin B and L activity.** For whole cell cathepsin activity, lymph node divested number four glands were snap frozen and ground to a fine powder in a mortar. Total protein was extracted with modified RIPA buffer (50 mM Tris, 1% NP40, 0.25% sodium deoxycholate, 150 mM NaCl, 1 mM EGTA and Pefabloc 1 mM (Fluka), at pH 7.4). To measure lysosomal and cytosolic cathepsin

activity, subcellular fractionation was carried out as described earlier. In both cases, protein levels were assessed with the BCA Protein Assay (Thermo Scientific) and equal amounts of protein (4  $\mu$ g) were added to a total of 200  $\mu$ l cathepsin reaction buffer (sodium acetate 50 mM, EDTA 8 mM, dithiothreitol 8 mM and Pefabloc subcellular fractionation buffer 1 mM, at pH6). Cathepsin B+L activity was measured after incubation (15 min, 37°C) with the fluorescent substrate Z-Phe-Arg-AMC (Calbiochem, 50  $\mu$ M) in a Synergy HT Multi-Detection Microplate Reader (Bio-TEK; excitation 380 nm, emission 442 nm). In parallel, a sample with added cathepsin B inhibitor CA-074 (Peptanova; 5  $\mu$ M) was measured to determine cathepsin L activity. The difference between readings corresponds to the cathepsin B activity.

**Caspase 3, 6 and 7 activity.** Caspase activity was measured with the fluorescent substrates AC-DEVD-AMC for caspases 3 and 7 and AC-VEID-AMC for caspase 6. Protein (100  $\mu$ g) was diluted in caspase reaction buffer (10 mM HEPES at pH 7.5, 50 mM NaCl and 8 mM dithiothreitol), and incubated with a final concentration of 50  $\mu$ M of the respective substrate. The samples were incubated at 37°C for 5 h and fluorescence was measured in a Synergy HT Multi-Detection Microplate Reader (Bio-TEK; excitation 380 nm, emission 442 nm).

**Quantitative real-time PCR.** RNA extraction, complementary DNA synthesis and quantitative real-time PCR were carried out as previously described<sup>44</sup>. Expression levels were measured for *cyclophilin a* (housekeeping gene), *cathepsin b*, *cathepsin l* and *spi2a* using the following primers: cyclophilin A forward, 5'-CCT TGG GCC GCG TCT CCT T-3', reverse, 5'-CAC CCT GGC ACA TGA ATC CTG-3'; cathepsin B forward, 5'-TCC TTG ATCC TTC TTT CTT GCC-3', reverse, 5'-ACA GTG CCA CAC AGC TTC TTC-3'; cathepsin L forward, 5'-ATC AAA CCT TTA GTG CAG AGT G-3', reverse, 5'-CTG TAT TCC CCG TTG TGT AGC-3'; Spi2A forward, 5'-TTT CCA GCA ACC TCT CAA GGC-3', reverse, 5'-CTG GGT GTG ATT GCC CAC ATA-3'. Primers were designed using the PrimerBank website (<http://pga.mgh.harvard.edu/primerbank/>).

**Immunoblotting.** Sample preparation and immunoblotting was carried out as previously described<sup>44</sup>. The following rabbit antibodies from Cell Signaling Technologies were used: anti-cleaved caspase 3 (9661), anti-cleaved caspase 6 (9761), anti-cleaved caspase 7 (9491), anti-caspase 3 (9665), anti-caspase 6 (9762), anti-caspase 7 (9492) and anti-phospho-Stat3 (Tyr705: 9131). The following antibodies from Abcam were used: rabbit anti-cathepsin B (ab33538), rat anti-LAMP2 (ab13524) and rabbit anti- $\beta$ -actin (ab8227). Other commercial antibodies used were: rat anti-cathepsin L (R&D Systems, MAB9521), mouse anti-Stat3 (BD Transduction Laboratories, 610190) and rabbit anti-pan-p85 (Millipore, 06-49 6, also detects p50 $\alpha$ /p55 $\alpha$  subunits). All antibodies were used at a standard dilution of 1:1,000. Secondary horseradish peroxidase (HRP)-conjugated antibodies were purchased from Dako.

**Immunohistochemistry.** Tissue sections were prepared as previously described<sup>44</sup>. For assessment of cathepsin localization on tissue sections, the background was reduced by incubating the sections in 0.1 M glycine in PBS (pH 7.4) for 20 min. Subsequently, the tissue was permeabilized with 0.1% saponin (Sigma) in PBS and blocked in 10% normal goat serum (Dako) in PBS, 0.01% saponin. Primary antibodies used were: rabbit anti-cathepsin B (Abcam, 1:100), rat anti-LAMP2 (Abcam ab13524, 1:100), and for the caspases 3, 6 and 7, cc3, #9661; cc6, #9761; cc7, #9491; all rabbit, all Cell Signaling Technologies and all at 1:100 dilution. Secondary antibodies used were Alexa Fluor 488 goat-anti-rabbit-IgG (Invitrogen, 1:500) and Cy3 goat-anti-rat-IgG (Invitrogen, 1:500). Nuclei were counterstained with Hoechst 33342 (Sigma, 1:1,000). The pictures were acquired on a Zeiss Axioplan 2 microscope with the ApoTome set-up for deconvolution microscopy. Mander's coefficient was determined using the ImageJ plug-in Mander coefficient by T. Collins. It was carried out on at least four z stacks with at least 15 cross-sections for every time point analysed. For tissue-culture samples, Eph4 cells were seeded on chamber slides (NUNC). Cells were fixed with 4% paraformaldehyde, permeabilized with 1% saponin in PBS and blocked in 10% normal goat serum (Dako) in PBS, 0.01% saponin.

**Cell culture.** Eph4 cells were seeded on plastic or chamber slides and grown in DMEM (Gibco) containing 10% FCS (Sigma). At 50% confluency, cells were stimulated with a final concentration of 25 ng ml<sup>-1</sup> recombinant mouse Oncostatin M (495-MO, R&D Systems) or carrier (0.0001% BSA in PBS). Medium was renewed every 48 h. For Stat3 inhibition, the small-molecule inhibitor S31-201 (50  $\mu$ M) was added alongside OSM.

**Treatment of cells with cycloheximide.** Eph4 cells were seeded on 25 cm<sup>2</sup> dishes (400,000 cells) in DMEM/10% FCS. The following day, cells were stimulated for 6 h with OSM (25 ng ml<sup>-1</sup>) and cycloheximide (Calbiochem, 10  $\mu$ g ml<sup>-1</sup>). Corresponding amounts of carriers (PBS with 0.0001% BSA) were used as control

treatments. After 6 h, the medium was aspirated, cells were collected in 1 ml of Trizol (Invitrogen) and mRNA was extracted and quantified.

**Quantification of cell death by flow cytometry.** EpH4 cells were seeded on six-well Nunclon  $\Delta$  Surface plates (Nunc, 100,000 cells per well) in DMEM, 10% FCS (Gibco/Sigma). Stimuli (OSM, R&D, 25 ng ml<sup>-1</sup>; CA-074Me, Sigma, 10  $\mu$ M; S3I-201, 50  $\mu$ M) were added in DMEM, 1% FCS, the following day and renewed after 48 h. Cells were collected and resuspended in 100  $\mu$ l Annexin V Binding Buffer (10 mM HEPES/NaOH at pH 7.4, 140 mM NaCl and 2.5 mM CaCl<sub>2</sub>) and subsequently stained for 10 min in the dark with 5  $\mu$ l of Annexin V-FITC (Gibco). Next, propidium iodide (Sigma, 10 ng ml<sup>-1</sup>) was added for 5 min. Cells were washed with Annexin V Binding Buffer, and resuspended in 500  $\mu$ l of Annexin V Binding Buffer. Two-colour flow cytometry was carried out on a CyAn ADP flow cytometer (DakoCytomation). Data analysis was carried out using the FlowJo software (Tree Star).

**Lysotracker Red staining.** Cells were seeded, grown and stimulated as described for the cell death assay. Subsequently, the cells were collected, resuspended in 1 ml culture medium and incubated for 5 min at 37 °C. LysoTracker Red DND-99 (Invitrogen, 100 nM) was added to the suspension and incubated at 37 °C in the dark for 30 min. Single-colour flow cytometry was carried out on a CyAn ADP flow

cytometer (DakoCytomation), and the data were analysed using the Summit 4.3 software (DakoCytomation).

**Statistical analysis.** Every experiment was carried out with at least three independent biological samples. Where appropriate, statistical significance was assessed with Student's *t*-test. The correlation between cathepsin B inhibition and delayed involution was assessed with the Pearson coefficient using Microsoft Excel.

38. Alonzi, T. *et al.* Essential role of STAT3 in the control of the acute-phase response as revealed by inducible gene inactivation [correction of activation] in the liver. *Mol. Cell Biol.* **21**, 1621–1632 (2001).
39. Selbert, S. *et al.* Efficient BLG-Cre mediated gene deletion in the mammary gland. *Transgenic Res.* **7**, 387–396 (1998).
40. Kuida, K. *et al.* Decreased apoptosis in the brain and premature lethality in CPP32-deficient mice. *Nature* **384**, 368–372 (1996).
41. Lakhani, S. A. *et al.* Caspases 3 and 7: key mediators of mitochondrial events of apoptosis. *Science* **311**, 847–851 (2006).
42. Zheng, T. S. *et al.* Deficiency in caspase-9 or caspase-3 induces compensatory caspase activation. *Nature Med.* **6**, 1241–1247 (2000).
43. Warley, A., Powell, J. M. & Skepper, J. N. Capillary surface area is reduced and tissue thickness from capillaries to myocytes is increased in the left ventricle of streptozotocin-diabetic rats. *Diabetologia* **38**, 413–421 (1995).
44. Khaled, W. T. *et al.* The IL-4/IL-13/Stat6 signalling pathway promotes luminal mammary epithelial cell development. *Development* **134**, 2739–2750 (2007).



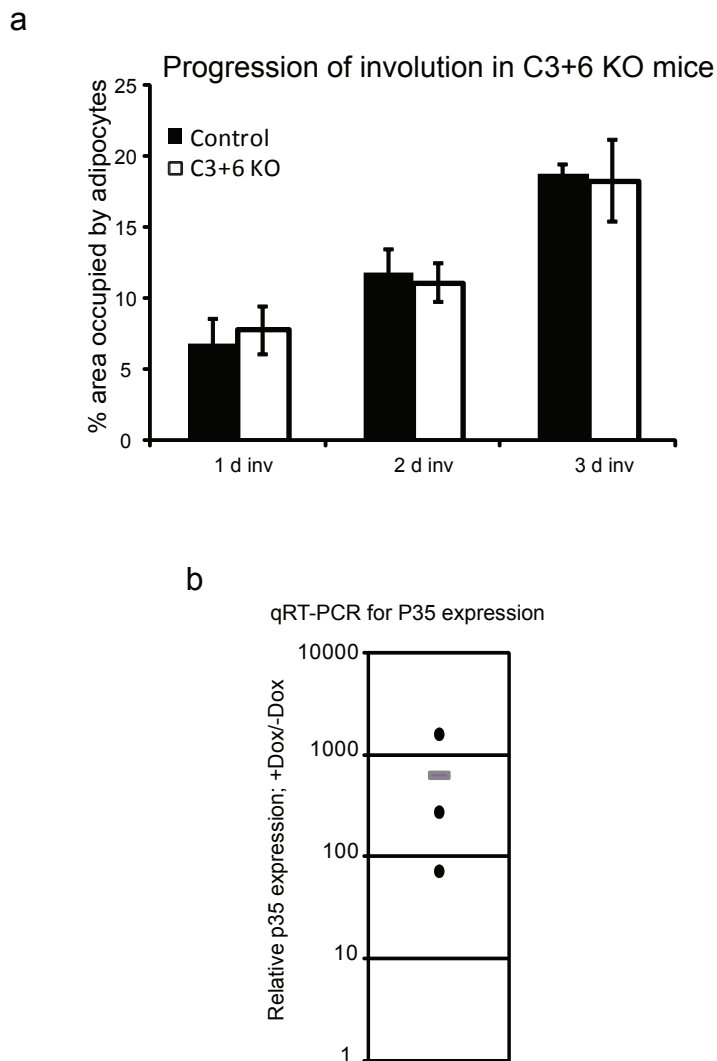


**Figure S2** Caspases are not required for involution. **a**, Measurement of the area occupied by adipocytes is a good indicator to assess the kinetics of involution. The area was measured using the imaging software ImageJ on at least five high power visual fields and shows that there is no significant difference between the caspase 3 and 6 double KO mice and control animals. For every time point three independent histological sections from three biological repeats were quantified. Values represent means  $\pm$  s.d. **b**, mRNA was harvested from mammary glands of bi-transgenic (rtTA/p35) mice

treated with systemic Doxycycline or untreated controls. Relative differences in p35 gene expression between paired (littermate) samples were calculated by using the  $2^{-\Delta\Delta CT}$  method, by normalising the CT values for each sample to the CT values for the beta-actin housekeeping gene. The average expression of p35 in control mice was set to 1 and the black dots represent fold increase of the p35 mRNA in each of three mice. The horizontal bar represents the average of these values. An average of 620 fold difference in p35 expression was observed.

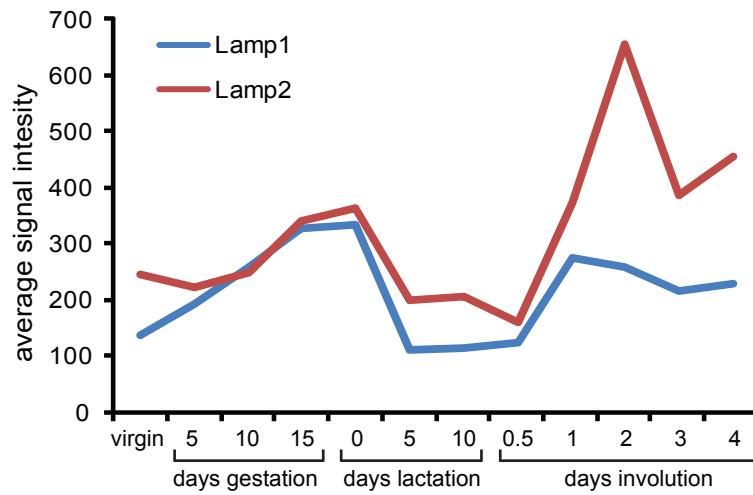


**Figure S3** LAMP1 and LAMP2 are transcriptionally down regulated during lactation. Microarray analysis of a 12 time point developmental time course of the mammary gland<sup>31</sup>. LAMP1 and LAMP2 are both transcriptionally down-regulated during lactation.

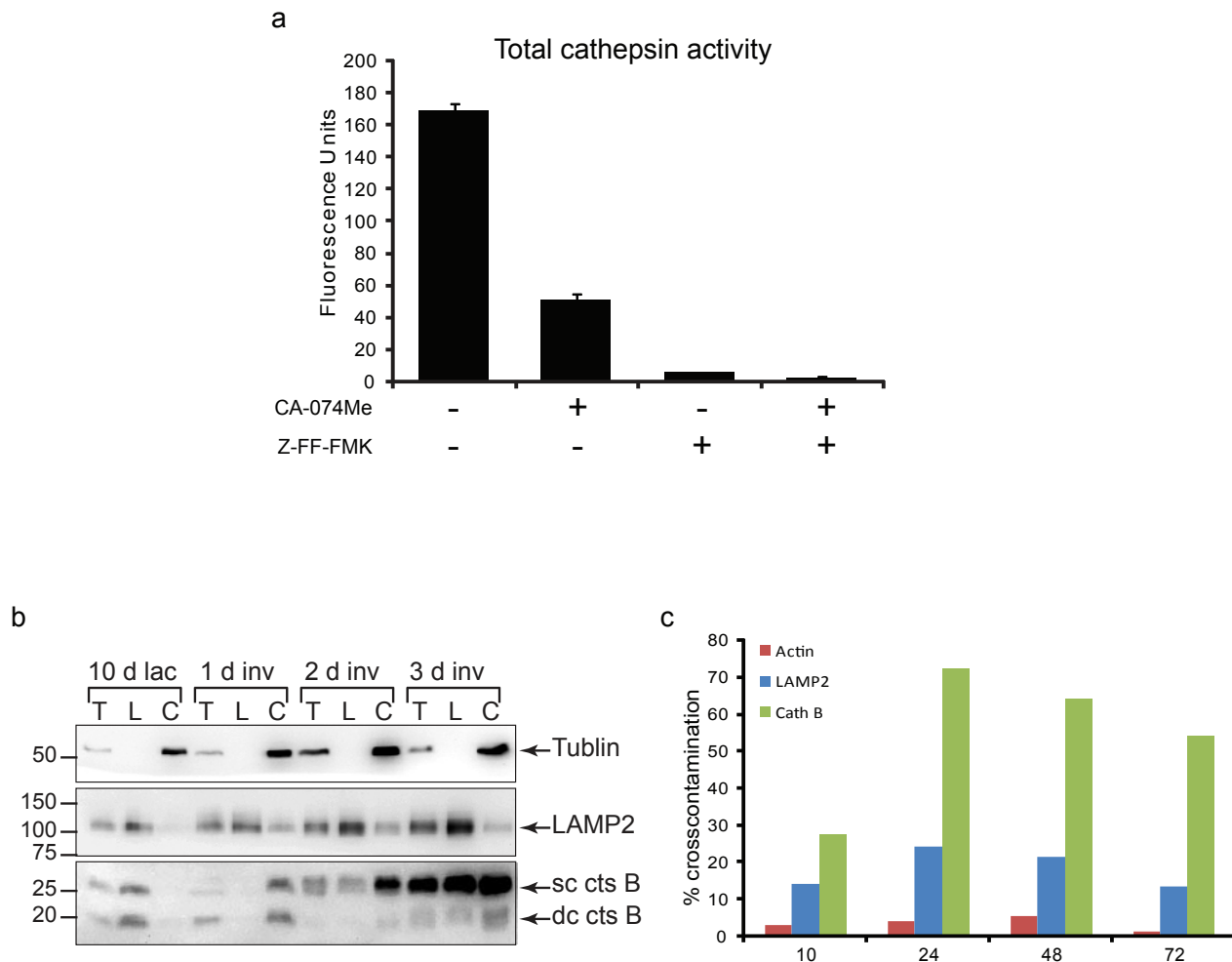


**Figure S4** Control assays for cathepsin activity measurement and tissue fractionation. **a**, The cathepsin like activity of tissue lysates from 2 day involution time points was measured with the addition of the cathepsin B inhibitor CA-074, the cathepsin L and partial cathepsin B inhibitor Z-FF-FMK (20 $\mu$ M, Calbiochem #219421) or both. Inhibition of both cathepsins left almost no residual cathepsin activity, demonstrating that the fluorescent substrate Z-Phe-Arg-AMC is almost exclusively cleaved by these cathepsins in our system (n=3, values represent means $\pm$ s.d.). **b**, The quality of the subcellular fractionation was assessed via western blot using specific

markers for the cytosolic (tubulin, rat, AbCam #6160) and the lysosomal (LAMP2) fraction (T=total lysate, L=lysosomal fraction, C= cytosolic fraction). Furthermore the distribution of cathepsin B was analyzed, showing a redistribution beyond levels of crosscontamination. The western blot was developed using the ChemiDoc imager (BioRad) and the supplied Quantity One software. This test was routinely performed and the samples are representative of a successful fractionation. **c**, The ratio of signal measured in the fraction in which the marker is not localized under normal conditions and the other cellular compartment. (i.e. for tubulin L/C).

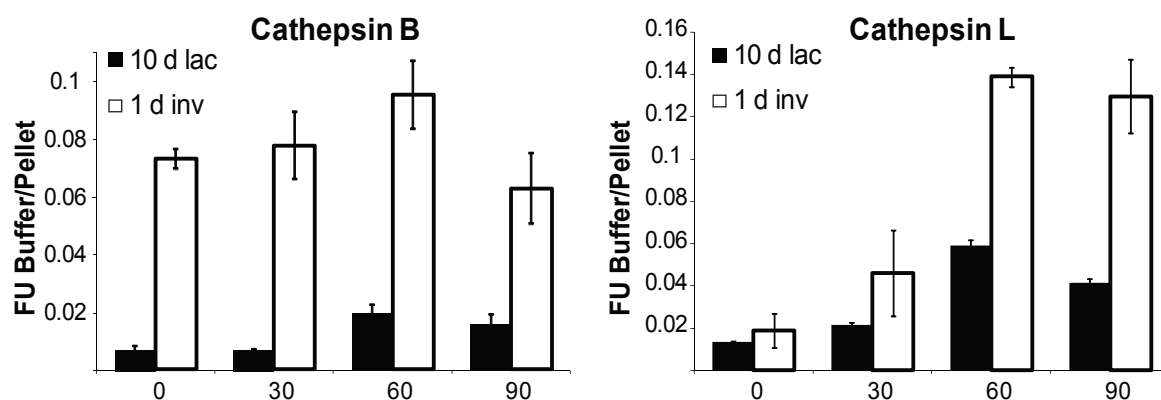


**Figure S5** Activity measurements show increased leakiness of lysosomes from involuting mammary gland compared to lactating gland. A lysosomal leakiness assay was performed as described, however using SC buffer rather than SC-PI to allow activity measurements. The cathepsin activity was measured in the pellet and the supernatant. To account for activity loss due to longer incubation periods, results are depicted as ratios of activity

in the supernatant and the lysosomal pellet. It can be seen that during involution significantly higher amounts of cathepsin activity are measured in the supernatant. The experiment was carried out six times for every time point consistently showing the same trend. The values stem from one representative assay and the error bars show the standard deviation from three independent repeats.

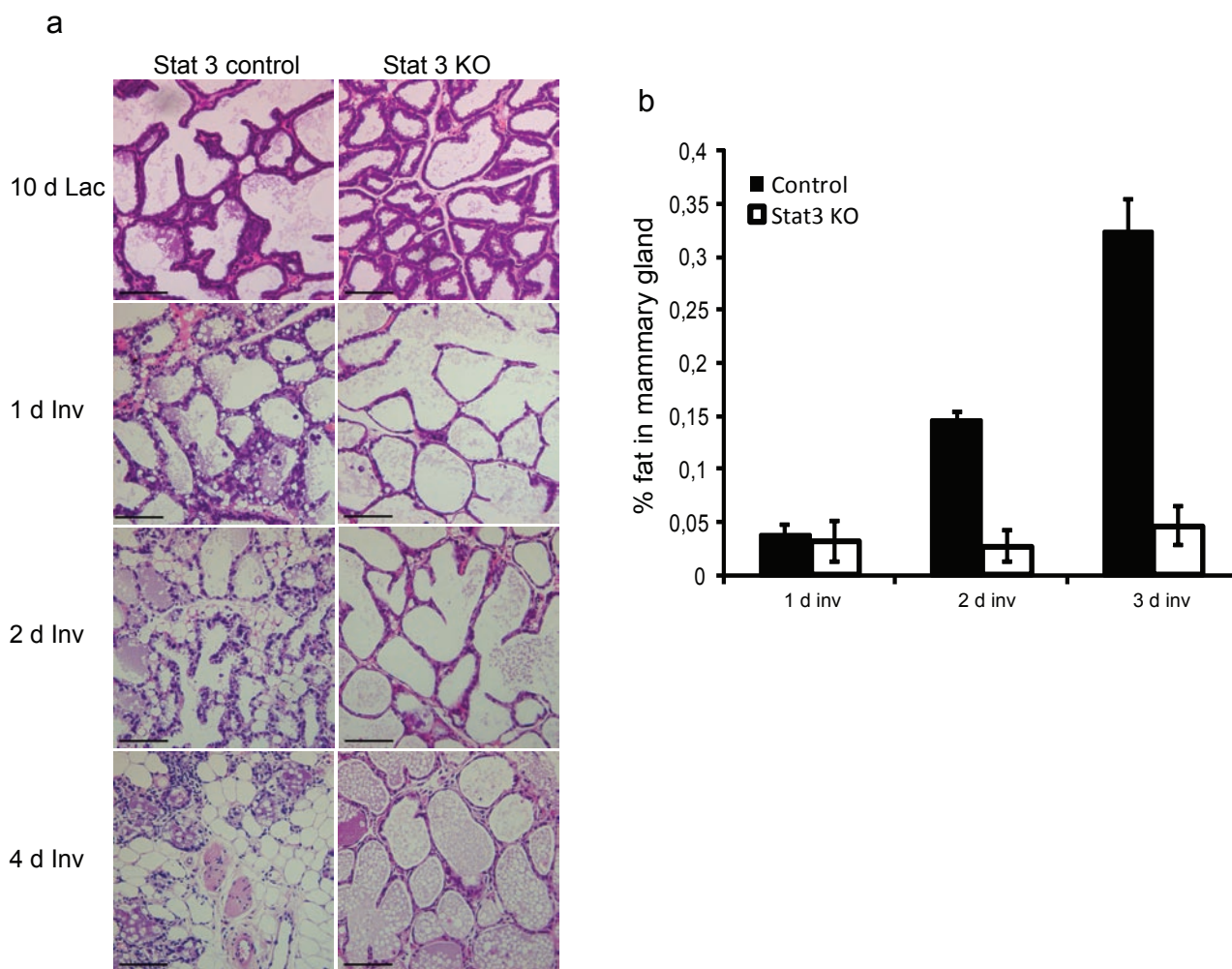


**Figure S6** Failed involution in the Stat3<sup>fl/fl</sup>, BLG-Cre mice. **a**, Histological confirmation of failed involution in mice with a conditional deletion of Stat3 in the mammary gland epithelium during lactation. Morphologically Stat3 KO mice are indistinguishable from the controls during lactation, but show little evidence of involution for a number

of days after weaning. Scale bars 100µm. **b**, The failed involution was additionally quantified by measuring the area repopulated by adipocytes as described above. For every time point three independent histological sections from three biological repeats were quantified. Values represent means±s.d.

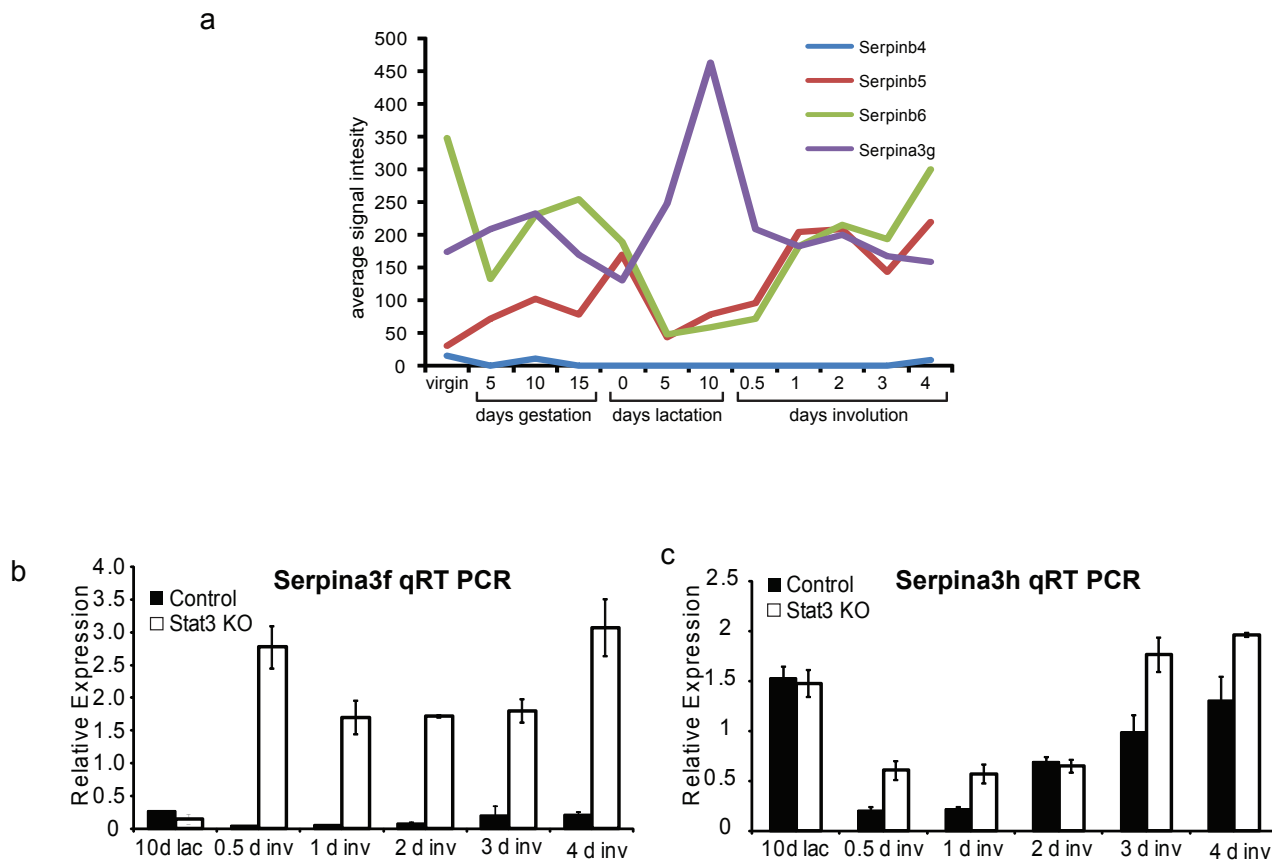


**Figure S7** Expression profile of selected serpins. **a**, Microarray analysis of a 12 time point developmental time course of the mammary gland. As opposed to the Clade A serpin Serpina3g, a number of Clade B serpins show low expression levels during lactation, while these increase in involution. Notably Serpinb4 shows almost no expression in the mammary gland. **b,c**, Quantitative real time PCR shows that Serpina3f, flanking Serpina3g upstream, is similarly over-expressed in the Stat3 KO mice. This is much

less striking for its downstream flanking neighbour Serpina3h. This shows a differential regulation of the Clade A locus. Primers used: Serpina3f Fwd, 5'-ATC TCC AAT GTT GTC AAG GTG-3'; Rev, 5'TGT AAC TTT TGC CAT AAA GAG-3', Serpina3h, Fwd 5'-CCA CAG GGG TCA AAT TAA TTC-3'; Rev, 5'-CTT GGG ATT TGT AAC TTT GGC-3'. Values represent means  $\pm$  s.d. of a representative time course and 3 independent mice have been studied for each time point.

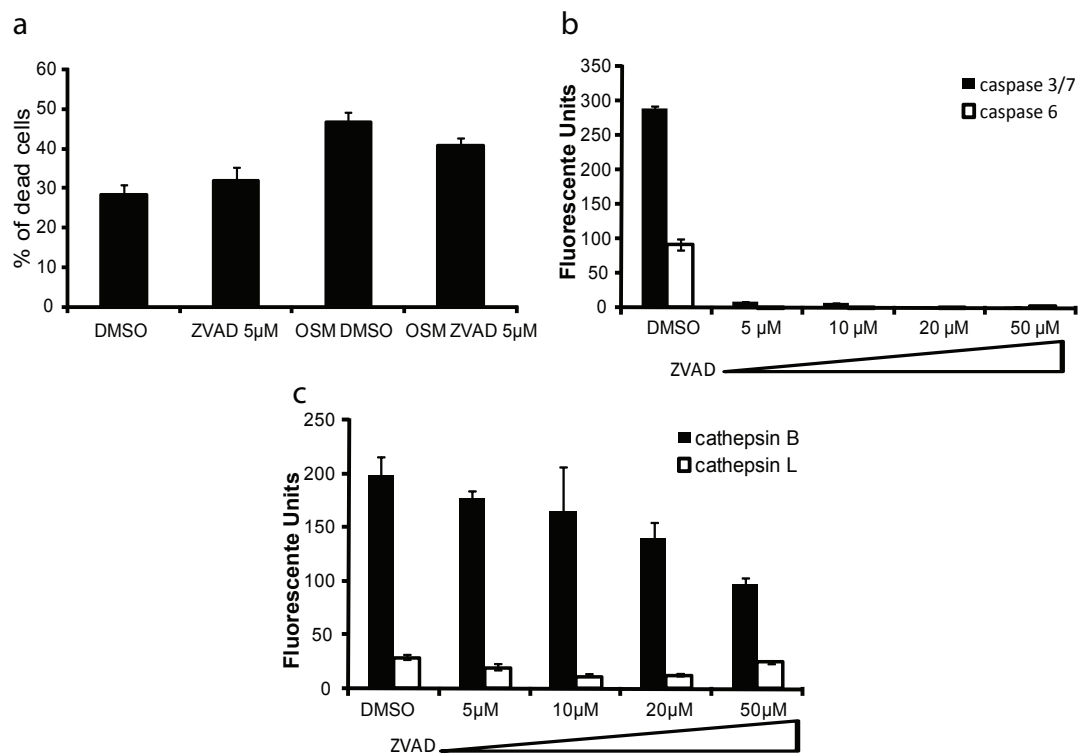


**Figure S8** Inhibition of caspases in OSM treated EpH4 cells has only a minor effect on cell death. **a**, Cell death assays were carried out as described in materials and methods, while cells were supplemented with the indicated amounts of the pan-caspase inhibitor Z-VAD-FMK (ZVAD, Sigma). Values represent means  $\pm$  s.d. of three independent biological repeats (n=3). **b**, **c**, Protease activity was measured as described in materials and methods.

Caspase 3 and 6 activities were measured after overnight incubation of 25µg at RT with the fluorescent substrates AC-DEVD-AMC (Sigma, 50 µM) and AC-VEID-AMC (Sigma, 50 µM), respectively. Inhibition of executioner caspases had only a minor effect on cell viability. Cathepsin activity was reduced by even low amounts of ZVAD, which could also influence cell viability. Values represent means  $\pm$  s.d. of three independent biological repeats (n=3).

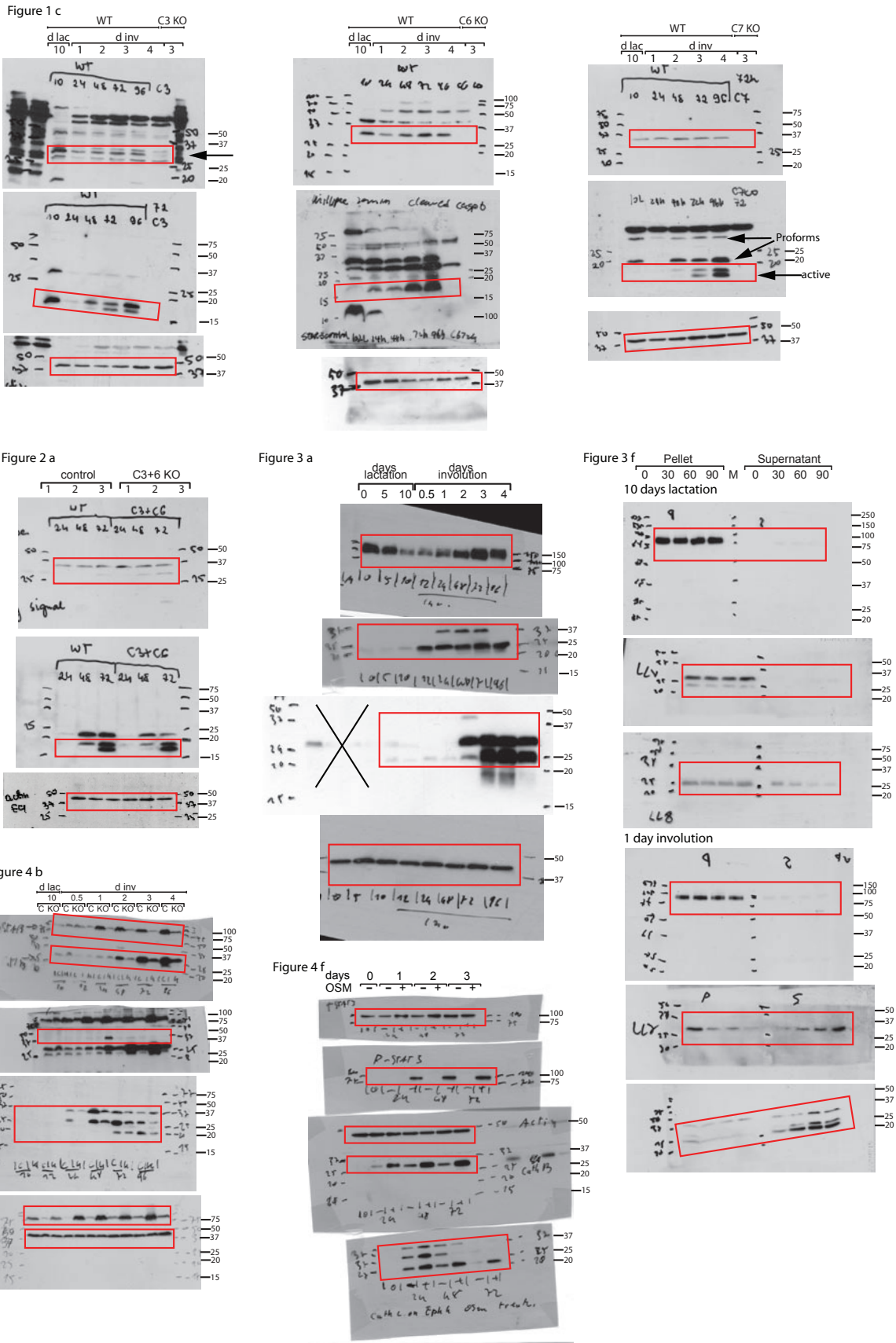


Figure S9 Uncropped western blots.

Figure Sg

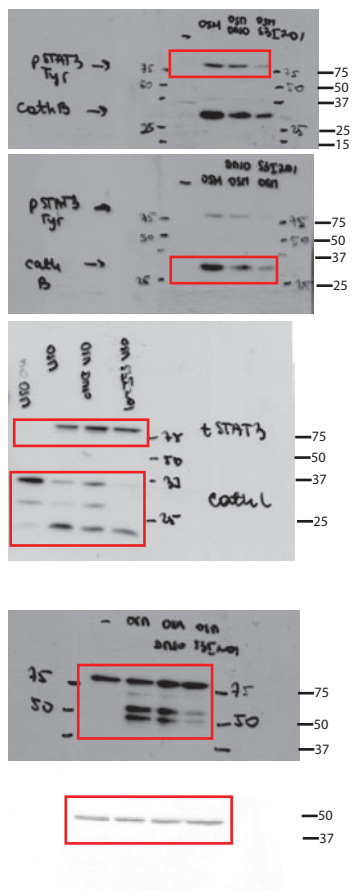


Figure S 4b

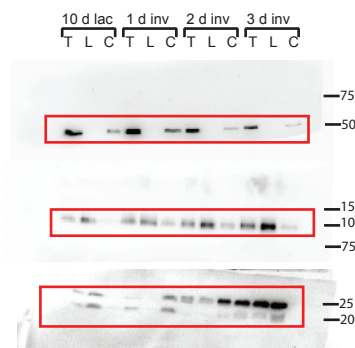


Figure S9 continued